UCRL-51868

SHOCK COMPRESSION PARAMETERS FOR A BORON-LOADED, SILICONE-RUBBER COMPOSITE

W. H. Gust
M. Van Thiel
G. R. Gathers

July 18, 1975

Prepared for U.S. Energy Research & Development Administration under contract No. W-7405-Eng-48

LAWRENCE LIVERMORE LABORATORY
University of California/Livermore

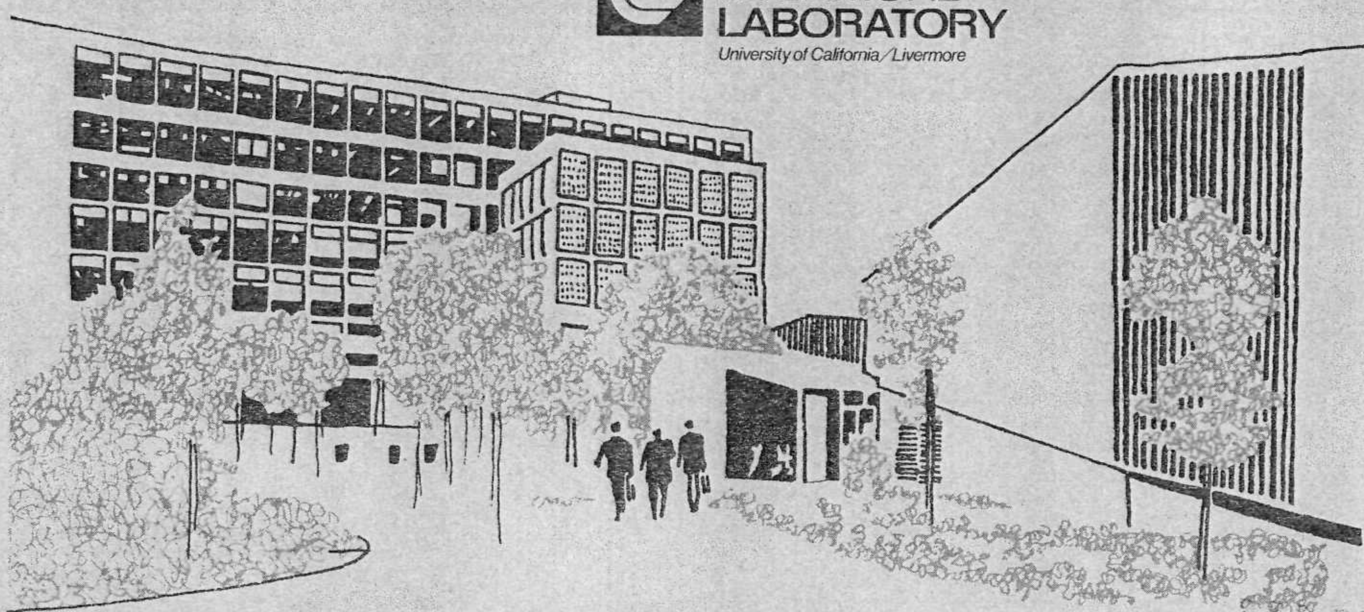

Distribution Category
UC-34

LAWRENCE LIVERMORE LABORATORY
University of California/Livermore, California/94550

UCRL-51868

SHOCK COMPRESSION PARAMETERS FOR A BORON-LOADED, SILICONE-RUBBER COMPOSITE

W. H. Gust

M. Van Thiel

G. R. Gathers

MS. date: July 18, 1975

DISCLAIMER

Contents

SHOCK COMPRESSION PARAMETERS FOR A BORON-LOADED, SILICONE-RUBBER COMPOSITE

Abstract

Hugoniot parameters under uniaxial-shock-wave-loading from 0.03 to 0.6 Mbar are presented for a composite with 70 weight-percent boron loaded in a silicone-rubber-matrix. The plot of shock velocity vs particle velocity was found to be non-linear. Equations which describe fits of the data are presented.

Introduction

The behavior of boron-loaded silicone-rubber is of interest because it is an efficient neutron absorber. The silicone-rubber provides an easily manufactured matrix in which a relatively high concentration of the neutron-absorber boron 10 can be uniformly dispersed.

Very little information concerning the equation-of-state properties of loaded-silastics is available. Mc Queen et al.[1] have measured the compression parameters for a quartz-loaded silicone-rubber, RTV-521. Nothing has been published for boron-loaded silastics.

We describe the results of shock-wave experiments on a silicone rubber loaded with 70 w/o boron These data provide values for some basic parameters needed for hydrodynamic calculations

Procedure

The explosive systems listed in Table 1 were used to generate plane shock waves producing pressures varying in the composite from about 0.03 to 0.6 Mbar. Data at pressures above 300 kbar were obtained using the flash-gap-technique; experiments at pressures less than 300 kbar were done with inclined prisms. Detailed descriptions of the experimental and data-reduction techniques may be found in Refs. 2 and 3. The data are reported in terms of pressure and volume where

$$P = \rho_o U_s U_p \quad \text{and}$$

$$V = \frac{U_s - U_p}{\rho_o U_s}.$$

The velocity of sound at high pressure was measured by a technique similar to the lateral relaxation method described

Table 1. Construction features of the shock generating systems used. (Shock generating systems consisted of a 0.3 m-diam-plane-wave lens with a 0.3 m-right cylinder of high explosive 0.15 m long unless noted otherwise. All attenuator components were flat and parallel within 5 μm.)

System	High explosive	Attenuator material	Component thickness-(mm)	Pressure in baseplate (+5%)(kbar)
A	Baratol[a]	Brass Lucite Al	25.4 12.7 12.7	63
B	Pressed TNT	Same as A	Same as A	100
C	Pressed TNT	Al	3.2	218
D	PBX 9205 (RDX)	Al	3.2	370
E	PBX 9404 (HMX)	Al	3.2	385
F	Pressed TNT	Air Brass Air Al	3.0 4.0 25.4 12.7	480
G	Pressed TNT	Air Monel Air Al	3.0 3.0 25.4 12.7	530
H	PBX 4205 (RDX)	Same as G	Same as G	680
I	PBX 9404 (HMX)	Same as G	Same as G	790

[a]H. E. cylinder was 0.10 m long.

by Al'tshuler.[4] In this method it is required that $\vec{C}_* + \vec{U}_p > \vec{U}_s$. When the shock passes through the baseplate-sample interface, a sound wave is initiated at the edge of the sample. It proceeds laterally through the compressed sample, and providing $\vec{C}_* + \vec{U}_p > \vec{U}_s$, it degrades the shock front in that region, thereby reducing the amplitude of the free-surface motion. The lateral penetration of the sound wave can be measured using a prism. To accomplish this, a flat prism was precisely placed so that the ends of the prism and the sample were aligned. Hence on the streaking camera record, the edge of the streak located the end of the sample. Further, the prism was long enough so that the shock profile caused by edge effects and a part of the undegraded shock could be observed.

Sound speed at high pressure is related to the shock parameters and the edge curvature through

$$C_* = U_s \left[(\tan \alpha)^2 + \left(\frac{U_s - U_p}{U_s} \right)^2 \right]^{1/2}$$

where

$$\tan \alpha = \frac{x_2 - x_1}{M\,h} \quad \text{(see Fig. 1).}$$

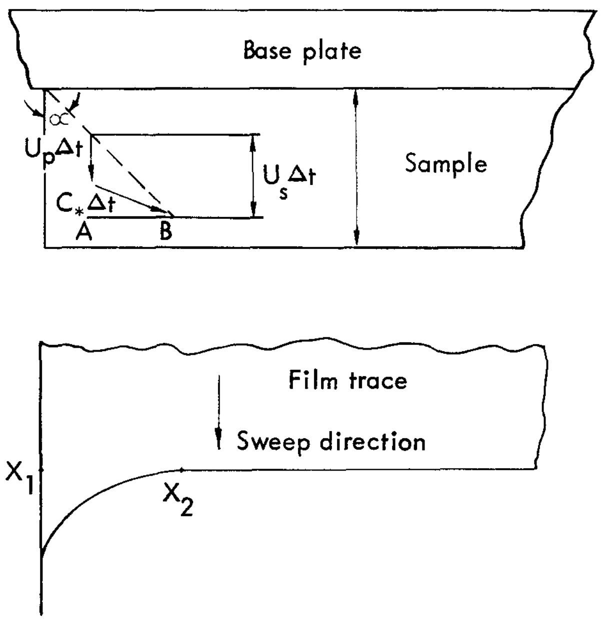

Here x_2 is the point of inflection on the film record where the undegraded shock profile merges with the curve caused by lateral sound wave penetration from the end of the sample. x_1 locates the end of the sample; this coincides with the edge of the streak. M is the image-magnification factor and h is sample thickness.

Fig. 1. Diagram of the relation between C_s and U_s. From the geometry it is seen that

$$\overline{AB} = U_s \Delta t \tan \alpha = \left[(C_* \Delta t)^2 - (U_s - U_p)^2 \Delta t^2\right]^{1/2}$$

$$C_* = U_s \left[(\tan \alpha)^2 + \left(\frac{U_s - U_p}{U_s}\right)^2\right]^{1/2} .$$

Materials

The samples were manufactured at Lawrence Livermore Laboratory (LLL). Standard rubber milling techniques[5] were used to uniformly disperse 70 w/o boron powder in a silicone-rubber matrix. The parts are roughly formed by cold molding and then subjected to a vulcanization procedure that included an applied pressure of 0.3 kbar for about 16 hr at 175°C. The end product should have a density of about 1.81 Mg/m^3.

Unfortunately, some of the samples tested were not subjected to the final vulcanization because of an oversight. Consequently there was considerable variation in density from batch to batch. Measured parameters for the low density samples are included, but must be used with caution.

Results

The Hugoniot parameters are listed in Table 2 and plotted in Figs. 2 and 3. The results indicate a non-linear relationship between shock and particle velocities. The longitudinal sound speed at one bar was 1.27 mm/μsec; no shear wave was observed. Sound speed in the compressed material was found to be described by $C_* = 1.42\, U_s - 1.37$.

Table 2. Data summary.

H. E. system	Free surface or shock velocity— (mm/μsec)	Pressure (Mbar)	Initial density, ρ_o (Mg/m^3)	Shock velocity U_s — (mm/μsec)	Particle velocity U_p — (mm/μsec)	Pressure (Mbar)	Volume (m^3/Mg)
A	0.83[a]	0.068	1.701	3.45	0.61[b] 0.56[c]	0.036 0.033	0.484 0.492
B	1.17[a]	0.10	1.704	4.42	0.80[b] 0.78[c]	0.060 0.059	0.481 0.480
C	2.26[a]	0.213	1.70	6.34	1.41[b] 1.66[c,d]	0.152 0.179	0.456 0.433
D	3.04[a]	0.310	1.705	6.66	1.90[b] 2.61[c,d]	0.215 0.295	0.421 0.358
E	3.36[a]	0.356	1.702	7.51	2.05[b] 2.24[c,d]	0.262 0.287	0.426 0.412
F	8.30[e]	0.507	1.765	7.79	2.69[b]	0.368	0.372
F	8.23[e]	0.490	1.795 1.625[f]	8.18 7.43	2.57[b] 2.73[b]	0.378 0.330	0.382 0.388
G	8.44[e]	0.540	1.799	8.35	2.74[b]	0.411	0.374
G	8.45[e]	0.540	1.785	8.32	2.76[b]	0.408	0.376
G	8.64[e]	0.585	1.788 1.636[f]	8.75 8.30	2.88[b] 3.01[b]	0.449 0.409	0.376 0.389
H	8.94[e]	0.664	1.779	9.12	3.15[b]	0.510	0.368
H	9.15[e]	0.720	1.775 1.625[f]	9.32 9.0	3.37[b] 3.49[b]	0.556 0.509	0.361 0.377
H	9.18[e]	0.743	1.780	9.20	3.38[b]	0.554	0.355
I	9.36[e]	0.776	1.765	9.13	3.58[b]	0.576	0.345
I	9.50[e]	0.818	1.789 1.566[f]	9.48 8.80	3.65[b] 3.91[b]	0.617 0.540	0.345 0.354

[a]Free surface velocity of Al.
[b]U_p from impedance match.
[c]$U_p = U_{FS}/2$.
[d]Disparity between U_p and $U_{FS}/2$, indicated jetting or spraying of silastics.
[e]Shock velocity of Al.
[f]Unvulcanized sample 3.2 mm thick.

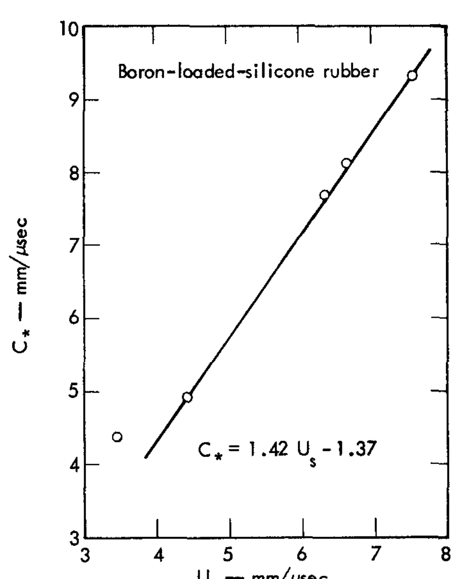

Fig. 2. The plot of C_* (sound speed at pressure) vs U_S (corresponding shock velocity). The large values for C_* indicate that the compressed composite behaves like a brittle material, i.e., more nearly like boron.

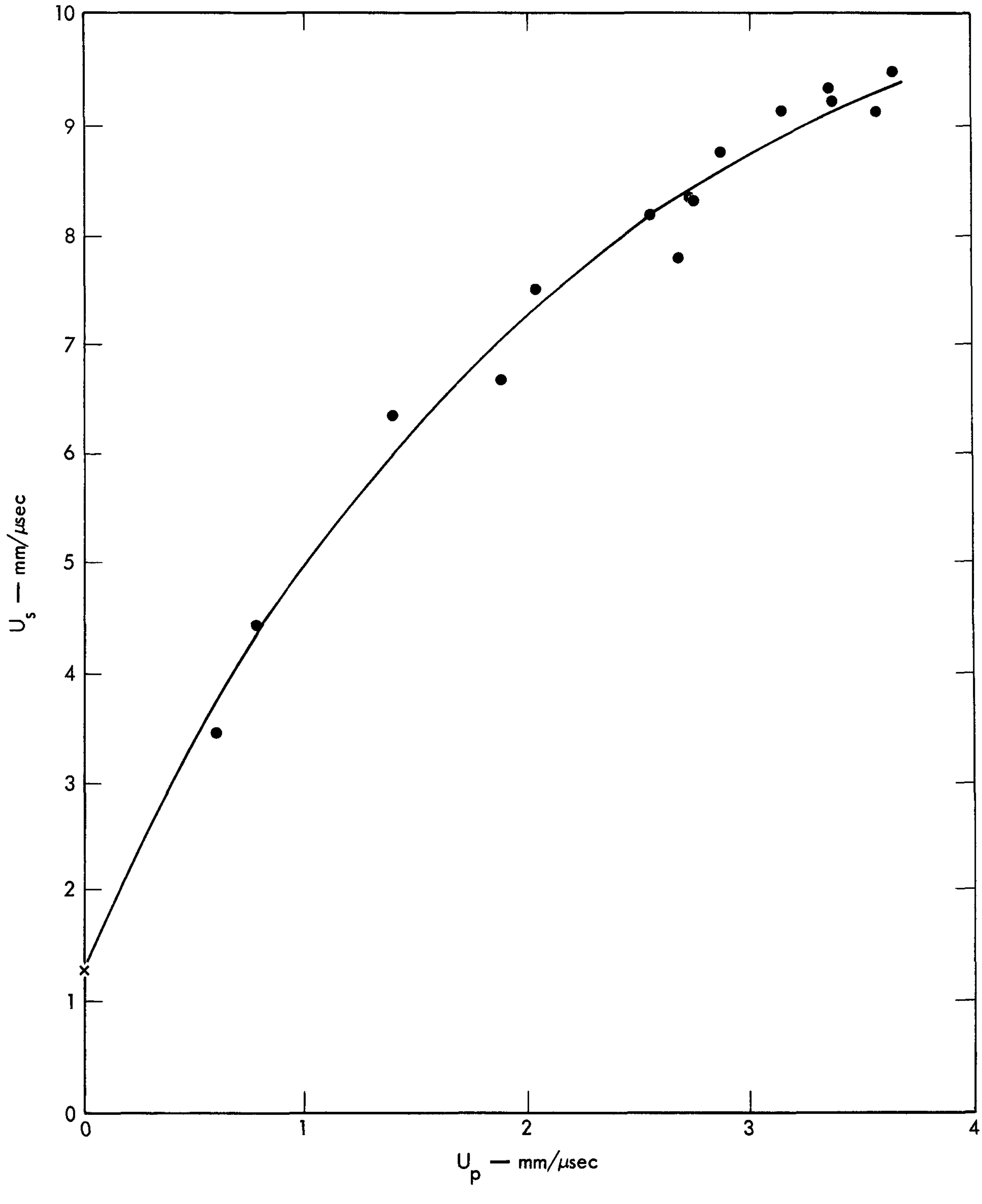

Fig. 3. Least-squares fit to the experimental data. The data display a nonlinear relation between shock velocity and particle velocity. The trace represents a constrained least-square fit to the data, namely

$$U_s = 1.27 + 6.33\ U_p - 1.59\left(\frac{U_p}{U_s}\right)U_p + 1.37\left(\frac{U_p}{U_s}\right)^2 U_p.$$

Discussion

The results indicate that boron-rubber exhibits several unusual features under shock loading. First, it is noted that values obtained for shock velocity indicate that the boron component of the compressed composite immediately dominates shock propagation. Shock velocities ranging from 4 to 9.5 mm/μsec are obtained at relatively low pressures. This is in contrast with the longitudinal sound speed at 1 bar, 1.27 mm/μsec, where propagation velocity is more consistent with

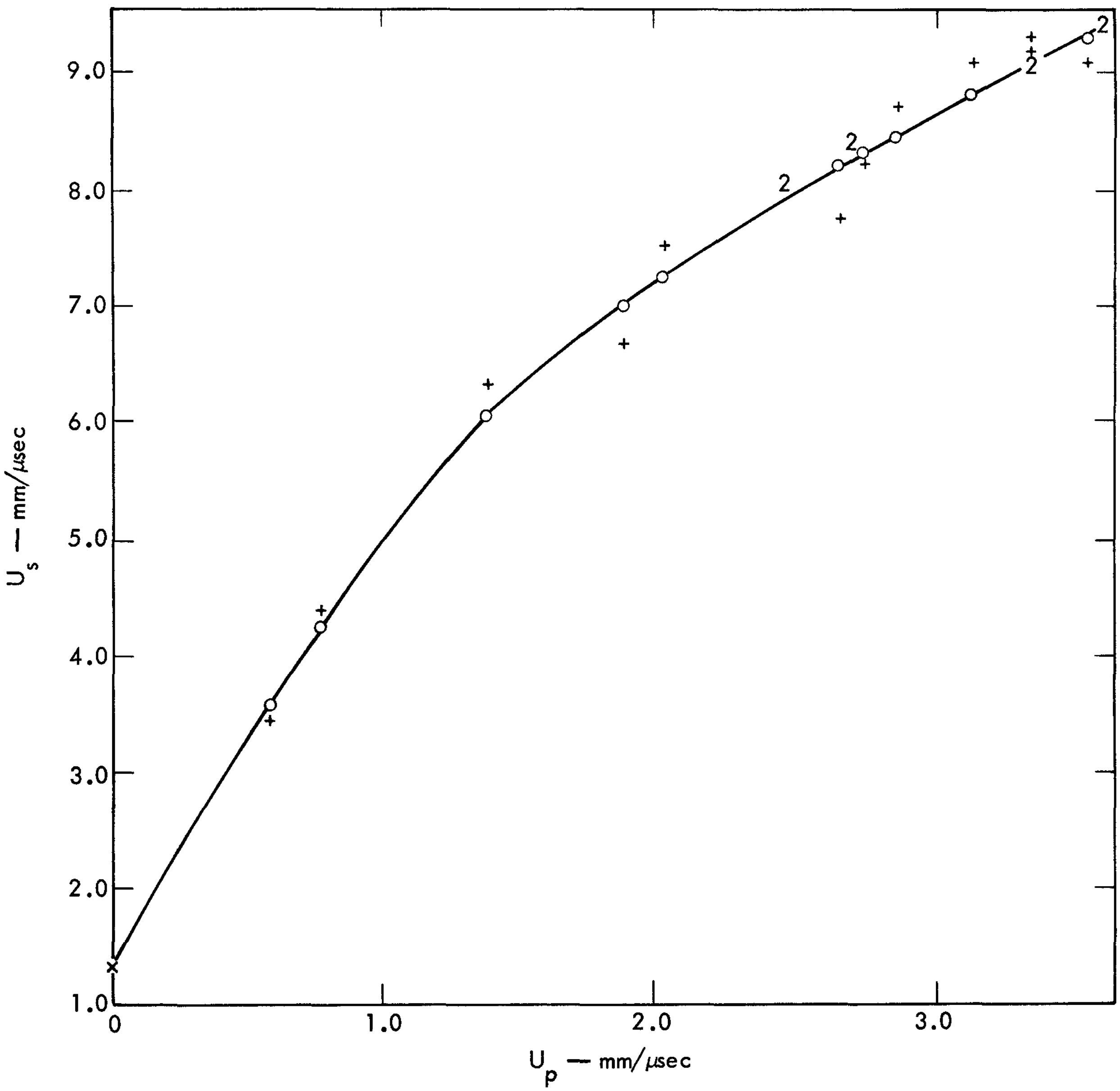

Fig. 4. Fit to Van Thiel's representation of the data. Here the same (U_s, U_p) data is fit to an equation

$$U_s = 1.27 + 5.62\left(\frac{U_p^{1.55}}{1 + U_p^{1.55}}\right) + 0.887\ U_p.$$

that of rubber. In other words, the material initially behaves like rubber, but under small pressure it immediately exhibits shock propagation qualities more like those of a brittle substance. Further, film traces from inclined prism experiments indicated high velocity jetting or spraying of one component, probably the silastic.

Additional evidence of anamolous behavior is obtained from the measurement of sound speed under compression. Figure 2 shows that sound speed in the compressed material immediately attains values greater than 5 mm/μsec. Note that the (C_*, U_s) curve does not intercept at the value for C_L at one bar, namely 1.27 mm/μsec, but at a negative value.

The least-squares fit coefficients for Grover's scheme[6] for obtaining a representation of non-linear (U_s, U_p) data are:

$$U_s = 1.27 + 6.33\,U_p - 1.59\left(\frac{U_p}{U_s}\right)U_p + 1.37\left(\frac{U_p}{U_s}\right)^2 U_p\,.$$

This constrained least-squares fit, based upon relative error is shown as the curve in Fig. 3.

Van Thiel has suggested that the initial non-linear portion of the (U_s, U_p) curve can be corrected by introducing an additional factor A ($U_p^n/1 + U_p^n$) in the usual linear equation. The optimum fit to the data for this type of representation (Fig. 4) was found to be

$$U_s = 1.27 + 5.62\left(\frac{U_p^{1.55}}{1 + U_p^{1.55}}\right) + 0.887\,U_p\,.$$

The standard deviation for U_s was 0.24 and the deviations for A and S were 0.48 and 0.14. This representation assumes continued linearity at very high pressures.

Acknowledgments

We wish to thank W. D. Barrowman for technical assistance, R. W. Brown, L. F. Simmons and A. Donnici for aid at the high-explosives test site, R. P. Brown for obtaining the materials, and D. I. Steinberg and Mark Wilkins for support.

References

1. R. G. Mc Queen, S. P. Marsh, J. W. Taylor, J. N. Fritz and W. J. Carter, High Velocity Impact Phenomena, Ray Kinslow, Ed. (Academic Press, New York, 1970) p. 356.
2. W. H. Gust and E. B. Royce, J. Appl. Phys. 42, 1897 (1971).
3. W. H. Gust and E. B. Royce, Phys. Rev. B 15, 8, 3595 (1973).
4. L. V. Al'tshuler, Usp. Fiz. Nauk 85, 197 (1965). [Eng. Trans. Soviet Phys. - USPEKHI 8, 52 (1965)].
5. Introduction to Rubber Technology, Maurice Morton, Ed. (Reinhold Publishing Corp., New York, New York) Ch. 16.
6. R. Grover, Lawrence Livermore Laboratory Internal Memorandum, STN 299 (1972). Readers outside the Laboratory who desire further information on LLL internal documents should address their inquiries to the Technical Information Department, Lawrence Livermore Laboratory, Livermore, California 94550.

TAL/bl/edas